Taylor & Francis
Taylor & Francis Group

Journal of the Air & Waste Management Association

ISSN: 1096-2247 (Print) 2162-2906 (Online) Journal homepage: http://www.tandfonline.com/loi/uawm20

Emission Strength Validation Using Four-Dimensional Data Assimilation: Application to Primary Aerosol and Precursors to Ozone and Secondary Aerosol

Alberto Mendoza-Dominguez & Armistead G. Russell

To cite this article: Alberto Mendoza-Dominguez & Armistead G. Russell (2001) Emission Strength Validation Using Four-Dimensional Data Assimilation: Application to Primary Aerosol and Precursors to Ozone and Secondary Aerosol, Journal of the Air & Waste Management Association, 51:11, 1538-1550, DOI: 10.1080/10473289.2001.10464380

To link to this article: http://dx.doi.org/10.1080/10473289.2001.10464380

Published online: 27 Dec 2011.

Submit your article to this journal

Article views: 56

View related articles

Citing articles: 6 View citing articles

Full Terms & Conditions of access and use can be found at
http://www.tandfonline.com/action/journalInformation?journalCode=uawm20

Download by: [University of North Texas] **Date:** 27 January 2017, At: 12:28

TECHNICAL PAPER

ISSN 1047-3289 *J. Air & Waste Manage. Assoc.* **51**:1538-1550
Copyright 2001 Air & Waste Management Association

Emission Strength Validation Using Four-Dimensional Data Assimilation: Application to Primary Aerosol and Precursors to Ozone and Secondary Aerosol

Alberto Mendoza-Dominguez
Chemical Engineering Department, Instituto Tecnológico y de Estudios Superiores de Monterrey, Monterrey, Mexico

Armistead G. Russell
Environmental Engineering, School of Civil and Environmental Engineering, Georgia Institute of Technology, Atlanta, Georgia

ABSTRACT

Three-dimensional air quality models (AQMs) represent the most powerful tool to follow the dynamics of air pollutants at urban and regional scales. Current AQMs can account for the complex interactions between gas-phase chemistry, aerosol growth, cloud and scavenging processes, and transport. However, errors in model applications still exist due in part to limitations in the models themselves and in part to uncertainties in model inputs. Four-dimensional data assimilation (FDDA) can be used as a top-down tool to validate several of the model inputs, including emissions inventories, based on ambient measurements. Previously, this FDDA technique was used to estimate adjustments in the strength and composition of emissions of gas-phase primary species and O_3 precursors.

In this paper, we present an extension to the FDDA technique to incorporate the analysis of particulate matter (PM) and its precursors. The FDDA approach consists of an iterative optimization procedure in which an AQM is coupled to an inverse model, and adjusting the emissions minimizes the difference between ambient measurements and model-derived concentrations. Here, the FDDA technique was applied to two episodes, with the modeling domain covering the eastern United States, to derive emission adjustments of domainwide sources of NO_x, volatile organic compounds (VOCs), CO, SO_2, NH_3, and fine organic aerosol emissions. Ambient measurements used include gas-phase inorganic and organic species and speciated fine PM. Results for the base-case inventories used here indicate that emissions of SO_2 and CO appear to be estimated reasonably well (requiring minor revisions), while emissions of NO_x, VOC, NH_3, and organic PM with aerodynamic diameter less than 2.5 μm ($PM_{2.5}$) require more significant revision.

IMPLICATIONS

Complex transport-chemistry air quality models are routinely used to investigate control strategy scenarios for reducing ground-level O_3, and models capable of following fine PM dynamics are increasingly being used. However, if such models employ a flawed emissions inventory, impact attribution analyses would suggest limited or improper conclusions. FDDA is an additional tool that modelers can use to assess the soundness of emissions inventories and to identify possible problems in the emissions inventory development process.

INTRODUCTION

As part of the U.S. Environmental Protection Agency's (EPA) reassessment of the National Ambient Air Quality Standards (NAAQS), revised standards for O_3 and particulate matter (PM) were promulgated in 1997. The standard for O_3 was modified, but perhaps the greatest impact to the regulated (and scientific) community came from the introduction of a new standard for PM with aerodynamic diameter less than 2.5 μm ($PM_{2.5}$). Even though the new $PM_{2.5}$ standard was remanded in 1999, it is not unlikely that a $PM_{2.5}$ standard will be part of the NAAQS in the near future, and visibility requirements impact $PM_{2.5}$ controls. The concern of air quality managers on the $PM_{2.5}$ standard is based on our poor understanding of this pollutant's emissions, physical and chemical dynamics in the atmosphere, and fate. The problem in understanding $PM_{2.5}$ dynamics relies in the complexity of the mechanisms by which it is formed and evolves in the atmosphere. $PM_{2.5}$ can have a primary pollutant component (e.g., emission of fine particles from combustion), but it is also generated in the atmosphere through gas-to-particle conversion processes. As part of an effort to better

characterize $PM_{2.5}$ levels in the atmosphere, instruments with the capabilities of measuring mass concentrations and chemical composition of $PM_{2.5}$ are being deployed, joining statewide ambient monitoring networks and the Interagency Monitoring of Protected Visual Environments (IMPROVE) monitors in various Class I areas. However, if a better understanding of the complex dynamics of PM in the atmosphere is to be attained, mathematical models and their inputs should also be improved.

Source-receptor relationships of PM in different locations (urban and regional) have been studied using empirical statistical models commonly known as "receptor models."[1] These models have proven to be valuable tools when applied to the inert portion of PM, and to some extent to secondary PM. Given that a significant fraction of $PM_{2.5}$ is secondary in origin, at least in some regions like the southeastern United States,[2] additional tools that describe the dynamics of aerosols in airsheds have been developed. Of particular interest are the extensions being made to current 3-dimensional Eulerian air quality models (AQMs) to include descriptions for photochemical smog and aerosols in the same model. These models represent the state-of-the-science in gas-phase and PM atmospheric modeling of urban and regional air pollution.[3] However, our understanding of the physical and chemical processes that govern aerosol dynamics still has limitations (as does that for O_3 and its precursors). Sources of uncertainty in model calculations include transport processes, numerical integration schemes, representation of chemical and thermodynamic mechanisms, errors in meteorological fields, definition of initial and boundary conditions, and emissions inventories.[4] This last component is viewed by some as the major source of uncertainty going into an application of an AQM.[5,6]

Different studies have suggested the use of inverse modeling as a top-down emissions inventory analysis tool for urban and regional domains.[7-11] This approach permits identifying plausible flaws in emissions strengths and misinventoried sources, and quantifies biases and uncertainties in the inventory.[3] In essence, inverse modeling incorporates into the traditional modeling effort information provided by ambient measurements. In particular, Mendoza-Dominguez and Russell[10] have developed an iterative 4-dimensional data assimilation (FDDA) approach for 3-dimensional AQMs that can be used for the purpose of emissions inventory validation. This FDDA technique has been applied to suggest adjustments in gas-phase emissions for the Atlanta nonattainment area.[11] In this paper, we present an extension to the same FDDA technique that also allows estimating adjustments for aerosol and aerosol precursor emissions. In addition, we apply the FDDA technique to analyze the emissions inventory for an area that covers the eastern United States and is centered around the southern Appalachian Mountains. Sources analyzed include domainwide categories of NO_x, volatile organic compounds (VOCs), CO, SO_2, NH_3, and fine organic aerosol emissions; ambient measurements include gas-phase inorganic and organic species and speciated $PM_{2.5}$. Emission scaling factors for two different modeling episodes (July 9–19, 1995, and May 22–30, 1995) are reported.

MODELING FRAMEWORK

The FDDA approach used here consists of a hybrid modeling system that combines a forward and an inverse model. The forward model provides simulated concentration fields of pollutants, and the response of those pollutant concentrations to changes in emissions. The inverse model estimates the changes in emissions necessary to bring simulated concentrations into closer agreement with actual observations. Given that the processes that govern pollutant dynamics in the atmosphere are nonlinear, iteration is used to get a stable response in the adjusted emissions. In this iterative process, the emission adjustments estimated by a given inverse model application are fed back to the forward model to obtain new fields of pollutant distribution and response fields to the new emissions for the subsequent inverse model application.

Mendoza-Dominguez and Russell[10] implemented this approach using the CIT (California/Carnegie Institute of Technology) airshed model[12] as the forward model and ridge regression as the inverse model.[13] The selection of ridge regression was based in part on its property of helping convergence in iterative estimation of nonlinear parameters.[10] The response of species concentrations due to changes in emissions is computed in an efficient way using a decoupled direct method (DDM-3D) sensitivity analysis module.[14] Their application demonstrated that three or four iterations are sufficient to obtain the final emission adjustments. However, a limitation of their application was that the model did not consider aerosol dynamics.

In this paper, we extend the application of the FDDA technique to determine aerosol and aerosol precursor emission adjustments. The AQM (forward model) used here is unique in that it forms part of an integrated atmospheric modeling system that combines gaseous, aerosol, and dry and wet deposition processes, incorporating also a direct sensitivity analysis technique. The major components of this modeling system include the Regional Atmospheric Modeling System (RAMS), version 3a[15] for estimating meteorological fields; the Emission Modeling System (EMS-95)[16] for emissions processing; and the urban-to-regional multiscale model (URM)[17,18] AQM for the modeling of pollutant transport and chemistry. Given the highly portable nature of the FDDA technique, the effort

needed to adjust the technique to use URM as the forward model from its previous applications using the CIT model was minimal. In fact, in principle, any AQM can be used with the FDDA technique as long as it can provide spatially and temporally varying concentration and sensitivity fields. Here, the most relevant features of the air quality component of the modeling system used are summarized, and the basis of the FDDA process is highlighted.

AQM

The URM model[17,18] is a 3-dimensional Eulerian AQM that accounts for the transport and chemical transformation of pollutants in the atmosphere. URM uses a finite element, variable mesh transport scheme in its horizontal domain to effectively capture the details of pollution dynamics at urban and regional scales without being computationally intensive.[19] Horizontal advection and horizontal diffusion are solved simultaneously using the 2-dimensional Streamline Upwind Petrov-Galerkin finite element method,[17,19] followed by application of a mass conservative diffusion filter.[20] Vertical advection is solved using first-order upwind differencing, while vertical diffusion is solved using an implicit finite difference scheme. Both vertical and horizontal diffusion are treated using K-theory. Mass conservation problems that arise in URM due to using RAMS wind fields (the two models use slightly different representations of the conservation equations) are minimized by adjusting the vertical velocities used by URM.[21]

URM has the capability of following both gas-phase and aqueous-phase atmospheric chemistry. Gas-phase reactions are modeled using the SAPRC chemical mechanism,[22,23] while aqueous-phase chemistry and cloud processes are based on the reactive scavenging module (RSM) of Berkowitz et al.[24] RSM simulates the time-dependent chemical kinetic interaction of clouds with the gas and aerosol species, as well as vertical convective transport within a column of air. Scavenging processes treated by the module include gas, aerosol, and microphysical scavenging. Further description of the coupling of RSM with URM can be found elsewhere.[25]

URM's aerosol module is capable of simulating concentrations of all major primary and secondary components of atmospheric PM. The continuous aerosol size distribution is modeled by a sectional approach. Here, four size bins are specified.[25] The aerosol module simulates mass transfer and particle growth occurring between the gaseous and aerosol species during condensation and evaporation, while effects of nucleation and coagulation are ignored.[25]

There are three groups of aerosol species that are considered: inert species, inorganic equilibrium species, and organic species. Inert species include Mg, K, Ca, elemental carbon, and a lumped category that includes all other inert PM species. The $Na\text{-}NH_4^+\text{-}Cl^-\text{-}SO_4^{2-}\text{-}NO_3^-\text{-}H_2O$ system is used to simulate the inorganic component of the aerosol. The physical state and composition of the inorganic fraction is computed using the thermodynamic equilibrium model ISORROPIA.[26] The organic aerosol fraction is represented by a lumped species, which is the sum of various condensable organics resulting from the oxidation of organic gases. The production of these condensable organic species is based on the organic yields reported by Pandis et al.[27] The formation of condensable organic aerosol species is computed in the chemistry module, followed by the distribution of condensed organic aerosols. Further details can be found in Boylan et al.[25]

Both dry and wet deposition processes are treated by URM. Removal by wet deposition is based on the parameterization in RSM as discussed earlier. Dry deposition is treated using a three-resistance approach based on the formulation of Wesely.[28] In particular, for aerosol particles, size-dependent deposition velocities were estimated.[25]

In addition to estimating pollutant concentrations, URM can calculate simultaneously their sensitivities to input data (e.g., emissions or meteorological fields) and model parameters (e.g., chemical reaction rate constants or deposition velocities). URM computes local sensitivity coefficients based on the direct decoupled method for 3-dimensional models (DDM-3D).[14] Sensitivities for gas-phase species are reported as ppm per percent change in a given model input or parameter (e.g., an emission source), while for aerosol species they are reported as $\mu g/m^3$ per percent change in the model input or parameter of interest. The integration of DDM-3D to the AQM is one of the features that allows fast convergence in the FDDA application.[11]

FDDA Extension

The FDDA technique integrates a 3-dimensional AQM (URM in this case), direct sensitivity analysis (DDM-3D), and a receptor analysis tool (ridge regression) to create a top-down emissions analysis tool. The objective of this approach is to estimate the amount emission strengths of diverse sources would need to be adjusted to minimize the difference between model-derived concentrations and actual observations. The inclusion of DDM-3D as part of the hybrid model makes the technique flexible enough to incorporate other inputs and parameters as the adjusted variables (i.e., changes in dry deposition parameters or initial and boundary conditions that minimize the discrepancy between simulated and observed concentrations could be estimated). However, for this particular application, we have limited the set of adjusted variables to certain emission source categories, implying that the main source of uncertainty in this case relies solely in the emissions inventory. We acknowledge that certain processes simulated, such as the organic yields that are used to derive the organic mass present in the aerosols, can have a

level of uncertainty similar to (or even greater than) the emissions. We have not intended to characterize the a priori uncertainty of each model component and input of the particular air quality modeling applications investigated here. The decision to use only emissions as adjusted variables is based on the current view that this is probably the most uncertain component in most air pollution modeling studies.[5,6]

The mathematical foundation of the FDDA method has been documented in detail elsewhere.[10,11] Briefly, the forward model (the AQM) provides information to the inverse model (ridge regression), which feeds back corrected emission estimates to the forward model. Here, URM (extended with DDM-3D) calculates simulated concentration and sensitivity fields in a single execution, and then these two fields, plus the relevant observations, are fed to a ridge regression module to estimate emission scaling factors of the emissions inventory used to drive the URM run. The ridge regression module solves the following linear system:

$$m = \left(G^{\mathrm{T}} W_{\mathrm{e}} G + W_{\mathrm{m}}\right)^{-1} G^{\mathrm{T}} W_{\mathrm{e}} d \qquad (1)$$

In eq 1, m represents the unknown vector of emission scaling factors, d is a vector of the difference between modeled and measured concentrations, and G is a matrix of weighted sensitivity coefficients (which indicate how the modeled concentrations vary as emissions are decreased or increased from a given base value). W_{e} is a weighting matrix that incorporates information regarding the uncertainty of the observations into the analysis, and W_{m} is an emission penalty matrix calculated based on the uncertainty in observations and the a priori and a posteriori uncertainty in the emissions. W_{m} is a diagonal matrix, and the magnitude of the terms in the matrix will indicate how much the emissions will be allowed to change from their base level. The penalty matrix helps to both constrain the emission estimates within prescribed bounds and improve convergence.[10] The complete formulation of how the W_{m} matrix is computed can be found elsewhere.[10,11]

The W_{e} diagonal matrix is computed as

$$\omega_{\mathrm{ik}} = \frac{1}{N_{\mathrm{i}}} \cdot \frac{1}{\sigma_{\mathrm{ik}}^2} \cdot \omega_{\mathrm{ik}}^{*} \qquad (2)$$

Note that in this notation, ω_{ik} represents the diagonal elements of the matrix W_{e} where the first k elements represent the k measurements corresponding to species $i = 1$, the next k elements represent the observations of the second species, and so on. N_{i} is the number of valid measurements of species i, σ_{ik} is the standard deviation of the kth measurement of species i, and ω_{ik}^{*} are additional weighting factors that are only used during the first two iterations to accelerate convergence.[10]

Finally, the way the G matrix is computed allows weighting how primary and secondary species will be used in the assimilation process. In essence, the sensitivity coefficients $s_{\mathrm{ik,j}}$ (species i sensitivity due to the emissions of source j at the position and time of the kth observation) used to assemble the G matrix are multiplied by a scaling factor, δ_{ij}. In our previous study,[11] the value of the scaling factor depended on whether species i was directly emitted by source j (in which case δ_{ij} had a value of 1) or not (in which case δ_{ij} was assigned a value of 0.5). This approach increased the sensitivity of an observed species to an emission category that emitted that same species, versus the weight given to other sensitivities (e.g., when adjusting for emissions of a NO_x source, the sensitivity of the simulated NO_2 concentration to that NO_x emission rate was given more weight than the sensitivity of, for example, CO to that same NO_x emission rate). This approach had the overall effect of stabilizing the response of the regression analysis.[11]

APPLICATION OF THE FDDA APPROACH

Modeling Domain and Grid

The modeling domain covers the eastern half of the United States and is shown in Figure 1. As noted previously, URM works with a single grid of variable resolution. The grid cell dimensions shown correspond to 192, 96, 48, 24, and 12 km with the finest resolution cells over the southern Appalachian Mountains. This domain is being used by studies assessing the effects of emission controls on air quality over the Class I areas around the southern Appalachian Mountains.[25,29] The domain extends from the surface to a

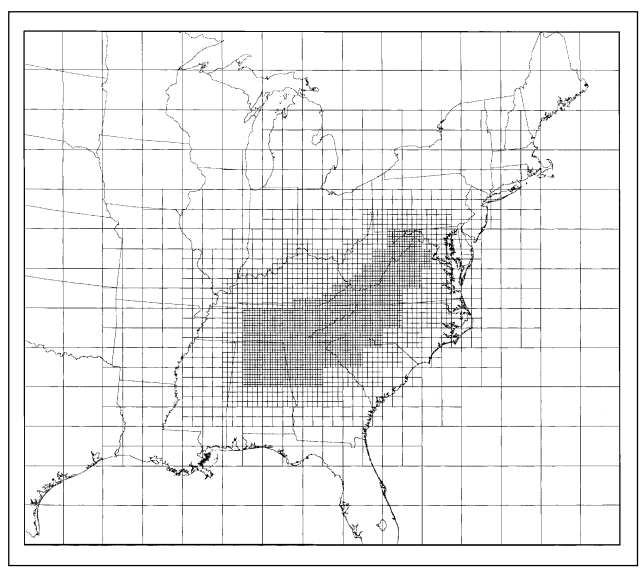

Figure 1. Modeling domain and the horizontal multiscale grid structure used by URM (the outer grids have a resolution of 192 km, while the innermost cells are 12 × 12 km).

height of 12,867 m above ground level and is divided into seven vertical layers. The thickness of each layer from the ground to the top of the domain is 19, 43, 432, 999, 1779, 3588, and 6007 m, respectively.

URM Inputs

Meteorological Fields. A modified version of the RAMS version 3a[15] was used to generate the meteorological fields required by URM.[29] RAMS was run with a system of three nested grids in a nonhydrostatic mode with cloud and rainwater modules activated (ice microphysics was not enabled).[29] The nested grid structure used in RAMS consisted of 96-, 24-, and 12-km-resolution grids, and the model was run under a one-way nesting mode. Some modifications in the version of RAMS used included cumulus parameterization and planetary boundary layer calculations (surface flux calculations), and are discussed by Odman et al.[29] The main source of data for initializing the RAMS runs and for nudging was the National Center for Environmental Prediction/National Centers for Atmospheric Research reanalysis data.[30]

Emissions Inventory. The EMS-95 framework[16] was used to generate gridded, time varying, and speciated emission inputs to be used by URM.[29] Emissions were generated for four major source categories: mobile, stationary, biogenic, and elevated point sources. Mobile emissions were estimated from the EPA MOBILE5b model. Biogenic emissions were obtained using the second version of the EPA Biogenic Emissions Inventory System (BEIS2).[31] The point source inventory includes day-specific emissions from power plants operating in the eastern United States. This would suggest that point-source SO_2 emissions should be reasonably well estimated. Meteorological model results obtained from the RAMS applications were also used to generate spatial and diurnal patterns of mobile and biogenic emissions.

Initial and Boundary Conditions. Initial (IC) and boundary conditions (BC) for gas-phase species were derived using data from the Aerometric Information Retrieval System (AIRS), while measurements from the IMPROVE network were used for defining speciated aerosol ICs/BCs.[25,29] IC/BCs for O_3, CO, and VOCs were generated by interpolating measurements to the modeling grid using Dirichlet tessellation (triangulated irregular network interpolation). In contrast, SO_2 and NO_x observations were interpolated using an inverse concentration, distance squared weighting of the natural logarithm of the concentrations to define their ICs/BCs. This minimizes and localizes the impact of locally high SO_2 and NO_x observations.[29] The values at the top of the domain were set to free troposphere values, and the values at intermediate layers were estimated by linear interpolation from the ground-level values to the top of the domain.

Episodes and FDDA Applications

Two high O_3/aerosol episodes were considered for the application of the FDDA technique: July 9–19, 1995, and May 22–29, 1995. The first 2 days in each episode were used as ramp-up days for the model simulation. Twenty observed species were assimilated for the July 1995 episode, and 17 for the May 1995 episode (Table 1). AIRS and IMPROVE databases were accessed to obtain the inorganic gas-phase species and aerosol species measurements, respectively. Photochemical assessment monitoring stations (PAMS) data were used to include VOC measurements. Adjustments for eight domainwide emission sources were estimated: anthropogenic area source NO_x (NO_x[A]), elevated point source NO_x (NO_x[P]), anthropogenic area source VOC (VOC[A]), biogenic VOC (VOC[B]), total SO_2 (SO_2[T]), total CO (CO[T]), total NH_3 (NH_3[T]), and total fine organic carbon PM (ORGF[T]). Anthropogenic area sources

Table 1. Observed species assimilated for the two 1995 episodes, and the coefficient of variation used for each species in the ridge regression module.

Species	No. of Observations[a]		Coefficient of Variation
	July 9–19, 1995	May 22–29, 1995	(%)
O_3	70,254	56,323	30
CO	36,111	27,357	50
NO	16,508	9936	50
NO_2	25,451	18,642	45
NO_x	11,434	8955	45
SO_2	59,030	42,296	40
Formaldehyde	240	–	50
Acetaldehyde	240	–	50
Acetone	240	–	50
Ethene	465	24	50
Isoprene	436	18	50
NMOC	192	24	50
SO_4^{2-} $PM_{2.5}$	19	19	30
NO_3^- $PM_{2.5}$	19	19	50
NH_4^+ $PM_{2.5}$	19	19	30
Crustal $PM_{2.5}$	19	19	60
Elemental carbon $PM_{2.5}$	19	17	40
Organic carbon $PM_{2.5}$	19	17	40
Total $PM_{2.5}$	19	19	30
Total PM_{10}	19	19	30

[a]Number of observations include only measurements reported by stations lying within the 12-, 24-, and 48-km grids.

included stationary, low-elevated point, nonroad, and mobile categories. Most of the SO_2 emissions in this domain come from elevated point sources (utility plants), while the largest CO contributors are mobile sources.

The adjustments considered here were estimated on an episode basis; that is, all episode observations were used to derive a single emission-scaling factor for each domainwide source category that applied to the whole episode. Daily assimilations (i.e., computing scaling factors for each source for each day of the episode) were beyond the scope of this work because aerosol and VOC observations were not available for all days of each episode. However, Mendoza-Dominguez and Russell[11] demonstrated that the FDDA technique is capable of computing emission corrections on a daily basis and for emissions located in particular subdomains of the modeling area. In computing adjustments on an episode and domainwide basis, we are also implicitly assuming that the temporal and spatial distribution of the emissions has less impact on the results than do the emission strengths.

Previous studies[10,11] that applied the FDDA technique assumed that inhomogeneities in the simulated concentration fields were not large, and comparing volume-averaged modeled concentrations to point measurements did not introduce large errors in the emission adjustment calculations. This assumption was based on the fact that the grid cells of the modeling domain used were relatively small (4×4-km square cells), and the concentrations fields in that region (Atlanta, GA) are expected to be smooth. However, these same arguments are not valid for the domain and grid structure used here. To take into account spatial inhomogeneities in the simulated fields, instead of using the variance of the observations in the W_e matrix (eq 2) as done in past studies, an estimated error based on the spatial inhomogeneities of the concentration fields was used. McNair et al.[32] describe a data-withholding technique that can be used to estimate spatial inhomogeneities in pollutant concentrations. However, the effort required to do a similar analysis in our domain becomes prohibitive. Based on the typical measurement errors found in the literature for the species assimilated in this work, the estimated relative lifetime of those species, and the trends suggested by the study of McNair et al.,[32] we derived a set of measurement standard deviations to be used in the W_e matrix. Table 1 indicates these standard deviations (as coefficients of variation). Results are not expected to be very sensitive to the magnitude of the standard deviations used.[11]

URM employs a multiscale grid that runs from 12- to 192-km-horizontal resolution, and it was considered that measurements taken in coarse cells would not be representative of the volume-averaged concentrations computed by the model. Thus, only observations taken by stations lying inside the 12-, 24-, and 48-km grids were considered. The total number of observations of these stations for each episode is summarized in Table 1. For the July 1995 episode, 131 AIRS stations with valid data were located in the 12-km grid, 220 were located in the 24-km grid, and 227 were located in the 48-km grid. For the May 1995 episode, 127 AIRS stations with valid data were located in the 12-km grid, 223 were located in the 24-km grid, and 226 were located in the 48-km grid. Similarly, IMPROVE measurements were used in the assimilation process.

Table 2 summarizes the IMPROVE stations used. Measurements from six stations from the PAMS network that measured speciated VOCs and total nonmethane organic compounds (NMOCs) were used for the July 1995 episode (see Table 2). Only one of these stations, Corbin, had valid VOC data for the May 1995 episode, and that was only for May 24. The six PAMS sites are located in the 12- and 24-km-resolution grids. Observations from five stations in the 48-km grid were available (one in Baltimore, one in the New York-New Jersey area, and three in the Philadelphia-Wilmington-Trenton area), but they were not used because these measurements could bias the FDDA results with northern urbanlike conditions in the case where the main interest are the rural regions of the southern Appalachian Mountains. The limited number of VOC observations and their poor spatial resolution had an important impact in defining the values assigned to the δ_{ij} scaling factors used to compute the G matrix (eq 1), as discussed in the next section.

Finally, a modification to the weighting matrix W_e was included to take into account the location where the measurements were taken in relation to the different grid resolutions. As mentioned, observations taken in the sections of the grid with resolutions of 12-, 24-, and 48-km

Table 2. URM grid resolution for IMPROVE (PM observations) and PAMS (VOC observations) stations.

IMPROVE Stations	Grid Cell Size (km)	PAMS Stations	Grid Cell Size (km)
Brigantine (NJ)	48	South DeKalb (GA)	12
Dolly Sods/Otter Creek (WV)	12	Conyers (GA)	12
Great Smoky Mountains (TN)	12	Fort Meade (MD)	24
Jefferson/James River Face (VA)	12	Aldino (MD)	24
Mammoth Cave (KY)	24	McMillan Reservoir (DC)	24
Cape Romain (SC)	48	Corbin (VA)	24
Shenandoah (VA)	12		
Shining Rock (NC)	12		
Sipsy (AL)	12		
Washington, DC	24		

were used in the assimilation process. However, the area covered by the 12-km grid represents an area of greater interest than the regions covered with coarser resolution grids, and those simulated data should be more comparable to the monitored data. Thus, a term to weight the relative importance of each measurement based on the grid resolution where the station is located was included in the calculation of the elements of the W_e matrix. Equation 2 was updated in the following manner:

$$\omega_{ik} = \frac{1}{N_i} \cdot \frac{1}{\sigma_{ik}^2} \cdot \frac{d_f}{d_{ik}} \cdot \omega_{ik}^* \quad (3)$$

where d_f is the resolution of the finest grid (i.e., 12 km) and d_{ik} is the resolution of the grid where the *k*th measurement of species *i* was taken.

RESULTS

In past applications[10,11] of the FDDA approach, all sources were treated simultaneously with all observations to obtain the estimated emission adjustment factors for those sources. In the applications reported in this paper, we observed instabilities in the estimated adjustment factors if the same approach is taken. Collinearity problems were observed, which resulted in problems with the inverse of $G^T W_e G + W_m$, especially in the first iteration steps. For example, inspection of the correlation matrix obtained from ridge regression in the first iteration step of the assimilation for the May 1995 episode data revealed off-diagonal terms with absolute values greater than 0.97. In particular, NO_x[A] and NO_x[P] were highly correlated with each other, as was VOC[A] with VOC[B] and ORG[T] with VOC[B]. This multicollinearity resulted in variance inflation factors (VIFs) for some regression estimates of 2 orders of magnitude higher than the ideal case value of 1. These high VIFs are an indication of low precision in the estimates.[33]

To overcome these difficulties, we treated separately each source in the first iteration steps; that is, the ambient measurements were used to estimate the emission adjustments of a single source, one source at a time. This alleviated the multicollinearity and stability problem, but induced at least two more iteration steps than the three or four previously[11] needed. The reason for the increment in the number of iterations is that a single source is adjusted to minimize the differences of all assimilated species without considering other sources. As iterations proceed, the adjustments of other sources redefine the direction toward which the single adjustments move.

In deriving the scaling factors reported in this work, the limited number of VOC measurements necessitated a different approach compared with our previous study[11] for defining the δ_{ij} values used to weight the sensitivity coefficients (to then construct the *G* matrix of eq 1). As described earlier, the δ_{ij} scaling factors were used before to emphasize the observations of primary species and allow the secondary species to refine the results. That approach is not viable in this study. Instead, secondary species such as O_3 were given more weight in trying to obtain stable adjustment factors.

A complete matrix of the values used for each δ_{ij} component is given in Table 3. In general, the VOCs were given less weight because of the lack of measurements, particularly being spatially sparse, to realistically reflect the variety of conditions in the airshed. In addition, VOC measurements were not used when the source was either VOC[A] or VOC[B] for the May episode (though VOC measurements were used with these sources in sensitivity tests discussed in the next section) because of the unrepresentativeness of these measurements. Measurements of NO and NO_2 were used only to constrain the NO_x sources (i.e., NO_x[A] and NO_x[P]); for all other sources, no significant differences were obtained using these measurements in addition to NO_x measurements. Even though elemental carbon and crustal $PM_{2.5}$ measurements were used, their influence on the results was negligible, as expected.

Some of the species were not assimilated because they resulted in severe instabilities of the adjusted estimates. In particular, for CO[T], the aerosol species (except the crustals and elemental carbon) affected this source unfavorably. In this case, the knowledge of the physics and chemistry of the model aids in concluding that this is probably a numerical artifact and these measurements do not provide relevant information on how CO sources should be modified. For the VOC sources, as for the NO_x sources, most of the weight was given to O_3 and NO_x measurements. As with CO[T], both VOC sources were also susceptible to instabilities when PM data were used, even when organic carbon $PM_{2.5}$ was assimilated. Here, it was assumed that allowing secondary gas-phase species to correct VOC emissions would also yield better estimates of secondary formation of organic aerosol. The implications of using the weighting scheme presented in Table 3 are further discussed in the next section.

Table 4 summarizes the results obtained from the AQM-FDDA application to the two episodes of interest. The values represent the scaling factors by which the domainwide emissions need to be multiplied to minimize the difference between observations and model predictions. As mentioned earlier, a single scaling factor was estimated for the emissions of the whole episode. Results from both episodes tend to be consistent with each other. Results indicate that the emissions of SO_2, CO, and NO_x from point sources are apparently well estimated using the conventional emission modeling techniques. The results obtained for SO_2 and NO_x[P] are an indication of the improved accuracy of emissions estimates

Table 3. Values defined for δ_{ij} in both model episodes.

Species	Sources[a]							
	CO[T]	SO_2[T]	NH_3[T]	NO_x[A]	NO_x[P]	VOC[A]	VOC[B]	ORGF[T]
CO	1.0	0.5	0.5	0.5	0.5	0.5	0.5	0.5
O_3	0.5	0.5	0.5	1.0	1.0	1.0	1.0	0.5
NO				0.5	0.5			
NO_2				0.5	0.5			
NO_x	0.5	0.5	0.5	1.0	1.0	1.0	1.0	0.5
SO_2	0.5	1.0	0.5	0.5	0.5	0.5	0.5	0.5
Ethene[b]	0.1	0.1	0.1	0.1	0.1	0.1	0.1	0.1
Isoprene[b]	0.1	0.1	0.1	0.1	0.1	0.1	0.1	0.1
Formaldehyde[c]	0.1	0.1	0.1	0.1	0.1	0.1	0.1	0.1
Acetaldehyde[c]	0.1	0.1	0.1	0.1	0.1	0.1	0.1	0.1
Acetone[c]	0.1	0.1	0.1	0.1	0.1	0.1	0.1	0.1
NMOC[b]	0.1	0.1	0.1	0.1	0.1	0.1	0.1	0.1
SO_4^{2-} $PM_{2.5}$		1.0	0.5	0.1	0.1			0.5
NO_3^- $PM_{2.5}$		0.5	0.5					0.5
NH_4^+ $PM_{2.5}$		0.5	1.0	0.1	0.1			0.5
Organic carbon $PM_{2.5}$		0.5	0.5	0.1	0.1			1.0
Elemental carbon $PM_{2.5}$		0.5	0.5	0.1	0.1			0.5
Crustal $PM_{2.5}$		0.5	0.5	0.1	0.1			0.5
Total $PM_{2.5}$		0.5	0.5	0.1	0.1			0.5
Total PM_{10}		0.5	0.5	0.1	0.1			0.5

[a]See text (p 1542) for description of abbreviations; [b]Factors for these species were assigned a value of 0 for the May 1995 episode (see text for details); [c]Species not measured during the May 1995 episode.

from using day-specific emissions available from continuous emissions monitors. (As noted previously, most SO_2 emissions in the domain come from utility emissions.)

Biogenic VOC emissions also appear to be well estimated. BEIS2 estimates for the southeastern United States have been found to closely represent real-world biogenic emissions in past studies,[11,34] and our results are in line with the results of those studies. Ground-level anthropogenic VOC and NO_x emissions, as well as NH_3 emissions, were the most frequently adjusted by FDDA to reconcile observations and model-derived concentrations. AQM studies in California's South Coast Air Basin[12,35] have reported that current mobile emission estimates might be understated by 2.5–3 times their real-world values, while others[6,36] have indicated the potential underestimation of NO_x mobile emissions (particularly from heavy-duty diesel vehicles). The results obtained here also suggest potential flaws in the VOC and NO_x inventory, though no differentiation was made between mobile and stationary sources.

DISCUSSION

Statistical model performance analysis is a basic tool used by air quality modelers to assess how closely the AQM is representing the atmospheric process in an airshed, and how suitable it is for considering its use to answer relevant scientific and environmental management questions.[37] Tables 5 and 6 summarize model performance results obtained for gas-phase and aerosol species, respectively, for the base-case simulations of the two episodes investigated. Even though this type of analysis can provide information regarding what sources might be misinventoried or biased, it cannot indicate how much, for example, the emissions should be adjusted to improve the model performance. Moreover, the biases themselves can be misleading in that attempting to reduce the bias of a certain species might negatively impact other species. The purpose of using FDDA is to have a formal methodology to

Table 4. Estimated emission adjustments for July and May 1995 base-case inventories (as scaling factors).

Source[a]	July 1995 Inventory	May 1995 Inventory
CO[T]	1.08	1.26
SO_2[T]	1.13	1.08
NO_x[A]	1.77	1.50
NO_x[P]	1.31	1.24
VOC[A]	2.21	2.84
VOC[B]	1.24	1.17
NH_3[T]	0.52	0.59
ORGF[T]	0.49	0.62

[a]See text (p 1542) for description of abbreviations.

Table 5. Gas-phase species model performance statistics for July and May 1995 base-case runs.[a]

Species	Mean Bias (ppb)	Mean Error (ppb)	Fractional Bias	Fractional Error	RMSE (ppb)	RMSEs (ppb)
	Statistics[b]					
July 11–19, 1995						
O_3	–4.00	13.9	–0.06	0.23	20.9	15.8
NO	–6.32	7.10	–1.17	1.29	17.4	17.1
NO_2	–6.54	11.4	–0.47	0.71	15.5	11.4
NO_x	–12.9	18.8	–0.55	0.77	29.8	26.2
CO	–369	473	–0.38	0.64	729	707
SO_2	–1.45	5.95	–0.07	0.87	12.6	10.7
Ethene	–0.09	0.99	–0.14	0.57	1.82	1.31
Isoprene	–0.06	2.22	–0.27	1.04	3.85	2.96
Acetone	–4.17	4.17	–1.40	1.40	4.58	4.58
Formaldehyde	–3.45	3.89	–0.41	0.47	4.89	4.82
Acetaldehyde	0.03	0.90	0.08	0.36	1.17	1.11
NMOC[c]	–33.2	46.8	–0.22	0.36	58.8	56.3
May 24–29, 1995						
O_3	–5.90	10.1	–0.13	0.21	15.7	11.2
NO	–4.63	6.18	–0.98	1.18	14.6	13.7
NO_2	–4.25	9.29	–0.36	0.64	12.9	8.6
NO_x	–8.88	15.3	–0.43	0.69	25.4	21.1
CO	–233	359	–0.20	0.56	584	564
SO_2	1.28	6.04	0.28	0.86	11.9	8.95
Ethene	–0.25	0.26	–0.62	0.65	0.28	0.27
Isoprene	0.45	0.79	0.26	0.58	1.00	0.57
NMOC[c]	–19.1	26.8	–0.22	0.45	42.6	42.0

[a]Cutoffs: NO_2—5 ppb, NO_x—5 ppb, NO—0.5 ppb, O_3—40 ppb; [b]Statistics are computed based on the residual $r_i = P_i - O_i$, where O_i and P_i are the ith observed and predicted concentrations, respectively. The mean bias is $1/N \cdot \Sigma r_i$, where N is the number of valid observation/prediction pairs and the summation runs from $i = 1$ to N. Similarly, the mean error is $1/N \cdot \Sigma |r_i|$, the fractional bias is $2/N \cdot \Sigma[r_i/(O_i + P_i)]$, the fractional error is $2/N \cdot \Sigma[|r_i|/(O_i + P_i)]$, and the RMSE is $[1/N \cdot \Sigma(r_i)^2]^{1/2}$. The systematic RMSE (RMSEs) is obtained from $[1/N \cdot \Sigma(\underline{r}_i)^2]^{1/2}$, where $\underline{r}_i = \underline{P}_i - O_i$, and $\underline{P}_i = a + bO_i$ (a and b are linear regression coefficients); [c]Statistics reported in units of parts per billion of carbon.

determine with some degree of certainty the most likely combination of adjustments that will improve the overall model performance and result in a model that represents more accurately the real chemical state of the airshed being analyzed.

After a stable response was obtained by the FDDA application, a second model performance evaluation was conducted and compared with the base-case performance. Tables 7 and 8 summarize the new statistics computed for each episode. In comparing Tables 5 and 6 with Tables 7 and 8, caution needs to be taken, because not all statistics reported represent a good index to measure the improvement after using FDDA. The comparison is presented because these statistics retain information pertaining to absolute differences and biases in the performance of the simulations with respect to certain species.

Another option would be to analyze the behavior of the objective function being minimized (the objective function is defined as: $\Gamma = e^T W_e e + m W_m m$, where $e = d - Gm$). However, this last analysis lumps together the errors of all species, not allowing a species-by-species analysis of remaining errors and biases. In addition, if the minimization was conducted only on the first term of Γ, the reduction in the value of the objective function could be implied from the values obtained for the root-mean-square error (RMSE) of each species, because minimizing the square error would also minimize the root square error. However, the second term induces some biasing in the ridge regression estimates (i.e., the components of the m vector) to obtain stable estimators with low variances under conditions of few or noisy data. This biasing can translate into a detriment of overall fit and lower coefficients of determination (R^2)[38] for some species. Because of this degradation in the overall fit, it is not unexpected to obtain a slightly higher RMSE for some species after the assimilation procedure. For this reason, the systematic portion of the RMSE, the RMSEs, is reported in addition to the RMSE because it contains information regarding systematic biases in the model results, and even if the RMSE increases slightly after the FDDA procedure, a reduction in the RMSEs would indicate better performance.[11]

Low values of the RMSEs would indicate that most of the variation in the observations has been addressed by the model, and the remaining error {the unsystematic RMSE [RMSEu = $(RMSE^2 - RMSEs^2)^{1/2}$]} would be an indication of random error. It can be noted also that in the statistics reported, the normalized bias and error (which are typically reported) were omitted, and instead the fractional bias and error are listed. Seigneur et al.[37] have indicated that the normalized bias and error tend to overemphasize overpredictions, leading to possible erroneous conclusions from the use of the cited normalized quantities. To overcome this limitation, the same authors suggest using the fractional bias and error, which are bounded quantities: the bias is in the range of ±2, and the error is always less than 2.

Tables 7 and 8 indicate an improvement in the performance of species such as O_3 and NO_x for both episodes. Modest improvements were obtained for other species, such as CO. This is an indication that adjusting episodic

Table 6. Aerosol species model performance statistics for July and May 1995 base-case runs.

Species	Mean Bias ($\mu g/m^3$)	Mean Error ($\mu g/m^3$)	Fractional Bias	Fractional Error	RMSE ($\mu g/m^3$)	RMSEs ($\mu g/m^3$)
	Statistics					
July 11–19, 1995						
SO_4^{2-} $PM_{2.5}$	–0.74	2.02	–0.12	0.27	2.63	1.89
NH_4^+ $PM_{2.5}$	0.63	0.83	0.25	0.35	1.06	0.76
NO_3^- $PM_{2.5}$	0.27	0.41	0.06	0.89	0.70	0.36
Organic $PM_{2.5}$	0.04	2.02	0.03	0.37	2.43	1.74
$PM_{2.5}$	–5.37	6.37	–0.22	0.27	8.03	6.73
PM_{10}	–2.46	7.71	–0.11	0.23	10.79	6.23
May 24–29, 1995						
SO_4^{2-} $PM_{2.5}$	–0.98	2.20	–0.20	0.36	2.74	2.59
NH_4^+ $PM_{2.5}$	0.83	0.91	0.37	0.44	1.18	1.09
NO_3^- $PM_{2.5}$	0.69	0.79	0.54	1.03	0.92	0.74
Organic carbon $PM_{2.5}$	–0.25	1.03	–0.01	0.28	1.25	1.08
$PM_{2.5}$	–2.82	5.09	–0.18	0.31	6.76	6.30
PM_{10}	–0.81	8.81	–0.04	0.35	10.3	8.39

domainwide emissions does not resolve all the possible sources of differences between model predictions and actual concentrations. In fact, this is not unexpected, because apparently we would be asking too much of FDDA to drastically improve the performance of all species at such time and spatial scales by scaling emissions only at the domainwide level. In addition, the statistics are episode averages for all the observations in the domain, and for some species the number of observations that go into the calculation of the statistics is significant. Thus, significant local improvements do not show in the analysis. Another alternative to improve the overall performance is to increase the temporal and spatial resolution used by FDDA. This implies, for example, adjusting for daily rather than episodic emissions[11] and partitioning the modeling domain in subdomains and computing adjustment for those areas separately.[7,11] However, the type of analysis conducted here is valuable in that, even though the temporal and spatial scales used for the computations were large, there exists evidence to indicate that the trends observed are significant. For example, CO, area source NO_x, and anthropogenic VOC emissions appear to have been understated in the base-case emissions inventories of both episodes. Taking this one step further, some might argue that increasing the resolution for the FDDA analysis would tend to overcorrect the emissions below the legitimate uncertainty expected from the model calculations.

Some emission sources were of particular interest in that the base-case model performance statistics suggested conflicting adjustment scenarios. For example, for the May episode, the performance for SO_2 in the base-case simulation suggests an overprediction, while the SO_4^{2-} $PM_{2.5}$ performance indicates an underprediction. The selection of the weighting scheme presented in Table 3 for the δ_{ij} weighting factors is clearly only one option of several that can be suggested. Thus, the impact of the values selected for these factors on the final

Table 7. Gas-phase species model performance statistics for July and May 1995 simulations after applying the adjusted emissions inventories.[a]

Species	Mean Bias (ppb)	Mean Error (ppb)	Fractional Bias	Fractional Error	RMSE (ppb)	RMSEs (ppb)
	Statistics					
July 11–19, 1995						
O_3	–0.02	15.2	–0.03	0.25	21.7	13.2
NO	–3.84	7.93	–0.75	1.11	18.7	15.8
NO_2	1.11	12.3	–0.06	0.60	17.8	8.40
NO_x	–1.95	20.1	–0.13	0.65	33.1	21.0
CO	–353	468	–0.35	0.63	723	697
SO_2	–0.53	6.09	–0.02	0.92	12.7	10.5
Ethene	4.83	5.10	1.14	1.18	6.78	5.02
Isoprene	0.44	2.55	–0.14	1.07	4.33	3.10
Acetone	–3.76	3.76	–1.16	1.16	4.21	4.20
Formaldehyde	–1.77	3.04	–0.16	0.34	3.87	3.69
Acetaldehyde	1.03	1.43	0.38	0.49	1.83	1.65
NMOC[b]	19.9	38.4	0.17	0.27	51.7	41.1
May 24–29, 1995						
O_3	–4.08	10.2	–0.10	0.22	15.9	9.90
NO	–2.77	6.81	–0.68	1.06	15.9	12.7
NO_2	0.41	9.95	–0.06	0.57	14.3	7.25
NO_x	–1.95	16.51	–0.11	0.62	27.9	18.2
CO	–198	353	–0.14	0.54	570	541
SO_2	1.95	6.45	0.36	0.88	12.3	9.09
Ethene	0.22	0.27	0.31	0.41	0.33	0.25
Isoprene	0.78	1.05	0.36	0.65	1.25	0.81
NMOC[b]	13.6	36.7	0.30	0.55	42.2	40.5

[a]Same cutoffs as in Table 5; [b]Statistics reported in units of parts per billion of carbon.

Table 8. Aerosol species model performance statistics for July and May 1995 simulations after applying the adjusted emissions inventories.

Species	Statistics					
	Mean Bias ($\mu g/m^3$)	Mean Error ($\mu g/m^3$)	Fractional Bias	Fractional Error	RMSE ($\mu g/m^3$)	RMSEs ($\mu g/m^3$)
July 11–19, 1995						
SO_4^{2-} $PM_{2.5}$	0.07	2.07	–0.05	0.26	2.73	1.95
NH_4^+ $PM_{2.5}$	0.13	0.61	0.08	0.28	0.80	0.44
NO_3^- $PM_{2.5}$	0.06	0.34	–0.60	1.14	0.55	0.25
Organic $PM_{2.5}$	0.66	2.09	0.14	0.36	2.69	1.99
$PM_{2.5}$	–4.65	5.87	–0.18	0.25	7.43	6.08
PM_{10}	–1.75	7.09	–0.08	0.21	10.11	5.28
May 24–29, 1995						
SO_4^{2-} $PM_{2.5}$	–1.10	2.08	–0.21	0.35	2.68	2.55
NH_4^+ $PM_{2.5}$	0.50	0.60	0.26	0.34	0.72	0.63
NO_3^- $PM_{2.5}$	0.46	0.64	0.16	1.02	0.80	0.58
Organic carbon $PM_{2.5}$	0.06	1.07	0.07	0.29	1.23	1.01
$PM_{2.5}$	–3.14	4.69	–0.19	0.29	6.40	6.00
PM_{10}	–1.17	8.44	–0.05	0.34	9.74	7.87

emission adjustments was further investigated.

To perform the analysis, once a stable response of the emission adjustment factors was obtained using the scheme presented in Table 3, some of the δ_{ij} were perturbed. The values set to 1 in Table 3 were kept as such, while the values set to 0.5 were decreased to 0.1. Under the alternative weighting scheme, the adjustment factors for May emissions of CO and fine organic PM were practically the same (1.27 and 0.60, respectively). The adjustment factors for SO_2, NO_x, and NH_3 emissions of the same episode changed somewhat: SO_2[T] was now decreased by 7% from its base value, NO_x[A] increased only by 44%, NO_x[P] increased by 35%, and NH_3[T] decreased by 50%. In this case, both NO_x emissions are still increased, but the relative amounts are different, with area sources still being corrected more than point sources.

The change in the estimated scaling of SO_2 emissions demonstrates that the procedure is sensitive to the relative importance that is given to each observed species, and a careful analysis of the observational data set being used is very important. For this species, it is apparent that, for example, in reducing the weight of total $PM_{2.5}$, the SO_2 observations could be outweighing the SO_4^{2-} $PM_{2.5}$ observations. In the case of the analysis presented for SO_2 during the May episode, it can be concluded that in general the average emissions are estimated closely to what it is expected to be their real value, although they might be slightly under- or overpredicted. To further illustrate the sensitivity on the weighting scheme used, the VOC[A] adjustment factor for the May episode was computed including observations of NMOCs and ethene. The sensitivities of NMOC and ethene concentrations to VOC[A] were scaled by a factor of 0.1 (i.e., their corresponding δ_{ij} was set to 0.1). This change produced a new adjustment for VOC[A] of only 1.78 times the base-case inventory instead of the 2.84 times reported earlier (see Table 4).

The new VOC[A] adjustment is not as large as before, even with such a small value assigned to the δ_{ij} of NMOC and ethene, because on an absolute scale, the sensitivities of NMOC and ethene to VOC[A] are larger than the sensitivities of O_3 and NO_x to VOC[A] and thus drive the correction of this source. This is clearly noted by indicating that the mean bias of ethene and NMOC with VOC[A] scaled by 1.78 was 0.0 ppb and –3.1 ppb C, respectively, that the RMSE was reduced from 0.3 to 0.2 ppb for ethene and from 42.6 to 39.4 ppb C for NMOC, and that the performance of O_3 was degraded. In contrast, mean bias and RMSE for the same species increased for the simulation with a scaling factor of 2.78 for VOC[A], while the performance of O_3 improved. For this last case, it can be argued that improving the performance of O_3 is a better approach than using the VOC observations, which are sparse for this particular application.

Finally, relationships between the O_3/NO_x/VOC and $NH_4^+/NO_3^-/SO_4^{2-}$ systems can be observed from the results obtained. For example, Tables 4, 5, and 7 suggest that the July episode is lower in NO_x than the May episode, but there is a higher negative bias of O_3 in May. Thus, to compensate for the O_3 bias in May, VOC emissions during this episode were increased more than in July. Of note, the emissions of fine organic PM had to be decreased in both episodes due to the increase in the organic load in the gas phase, which generated more secondary organic aerosol. In both episodes, the NH_3 emissions were reduced from their base-case level due to high concentrations of NH_4^+ aerosol. It was also observed that the decrease in gas-phase NH_3 contributed to lower concentrations of NO_3^- aerosol. In this case, NH_3 is being tied up with SO_4^{2-} to form $(NH_4)_2SO_4$, and not as much NH_3 remains to neutralize gas-phase HNO_3 to form NH_4NO_3. Observations of NH_3 and HNO_3 would be valuable to have a better picture of these last relationships.

In summary, the results presented here indicate that for the base-case inventories used here, emissions of SO_2 appear to be estimated reasonably well, while NO_x, VOC, NH_3, and organic $PM_{2.5}$ emissions require revision.

These results arise from the premise that emissions were the major source of uncertainty in the modeling exercise. Additional confidence in the SO_2 emissions is gained by the fact that day-specific emissions were used and to some extent the SO_2/SO_4^{2-} system is well known. On the other hand, caution should be taken with the results obtained for the organic portion of the $PM_{2.5}$, because this system is less well known and uncertainties in other model components may influence the results. In addition, the values presented in Table 4 should not be viewed as the "true" scaling needed to apply to the emissions. These values are estimates based on the assumptions described throughout the paper. However, and as mentioned earlier, there is confidence that the results can be taken as a guideline to improve the inventories used here, and overall that the technique is a valuable tool for similar analysis on other domains with their particular inventories.

CONCLUSIONS

The wealth of information contained in chemical measurements of the atmosphere is increasing as more and better analysis tools are becoming available. Moreover, the amount of observational data has increased immensely due to the deployment of more stations and instruments that enhance the capabilities of current routine networks. This trend will continue, particularly as satellite-derived data of atmospheric chemical composition become available, which would enable researchers to deduce 2- and 3-dimensional observed concentration fields. In this work, we have used FDDA as a means to incorporate ambient measurements to identify possible errors in the emissions inventory used in two air quality modeling episodes that had the eastern United States as the modeling domain. The FDDA approach consists of an iterative optimization procedure in which an AQM is coupled to an inverse model, and adjusting the emissions minimizes the difference between ambient measurements and model-derived concentrations. The FDDA technique used has the capability of assimilating both gas-phase and aerosol observed species.

Ambient measurements of gas-phase inorganic and organic species and speciated $PM_{2.5}$ were assimilated to derive emission adjustments of different sources of NO_x, VOCs, CO, SO_2, NH_3, and fine organic aerosol emissions. Results indicate that for the base-case inventories used here, emissions of SO_2 appear to be estimated reasonably well (requiring minor revisions), while NO_x, VOC, NH_3, and organic $PM_{2.5}$ emissions require revision (or other model components that can be responsible for the errors observed). The CO emissions appear to be somewhat underestimated. Even though a single correction factor per source for the whole episode was estimated, results are consistent between episodes and within each episode. No major difference was observed in the statistical model performance evaluation of some species before and after the assimilation was conducted, but this may be due in part to using a single factor for correcting emissions domainwide. Finally, it was also demonstrated that while the choice of weighting parameters in the FDDA application affects the adjustment factors obtained, the ultimate adjustments remained similar. A priori knowledge of the quality of the observations and the problem at hand should be used to define the strategy of assimilation that gives the most significant results.

ACKNOWLEDGMENTS

This study was supported in part by the U.S. National Science Foundation (Contract No. BES-9613729) and Georgia Power. A. Mendoza-Dominguez also acknowledges the Consejo Nacional de Ciencia y Tecnología (Mexico) for partial support during his research stay at Georgia Institute of Technology. The authors acknowledge the Southern Appalachian Mountain Initiative (SAMI) atmospheric modeling group for providing the air quality model input files used in this work.

REFERENCES

1. *Receptor Modeling for Air Quality Management*; Hopke, P.K., Ed.; Elsevier Science: Amsterdam, 1991.
2. Parkhurst, W.J.; Tanner, R.L.; Weatherford, F.P.; Valente, R.J.; Meagher, J.F. *J. Air & Waste Manage. Assoc.* **1999**, *49*, 1060-1067.
3. Seigneur, C.; Pai, P.; Hopke, P.K.; Grosjean, D. *Environ. Sci. Technol.* **1999**, *33*, 80A-86A.
4. Russell, A.; Dennis, R. *Atmos. Environ.* **2000**, *34*, 2283-2324.
5. Placet, M.; Mann, C.O.; Gilbert, R.O.; Niefer, M.J. *Atmos. Environ.* **2000**, *34*, 2183-2204.
6. Sawyer, R.F.; Harley, R.A.; Cadle, S.H.; Norbeck, J.M.; Slott, R.; Bravo, H.A. *Atmos. Environ.* **2000**, *34*, 2161-2181.
7. Mulholland, M.; Seinfeld, J.H. *Atmos. Environ.* **1995**, *29*, 497-516.
8. Haas-Laursen, D.E.; Hartley, D.E. *J. Geophys. Res.* **1996**, *101* (D17), 22823-22831.
9. Chang, M.E.; Hartley, D.E.; Cardelino, C.; Haas-Laursen, D.; Chang, W-L. *J. Geophys. Res.* **1997**, *102* (D13), 16023-16036.
10. Mendoza-Dominguez, A.; Russell, A.G. *Environ. Sci. Technol.* **2000**, *34*, 4974-4981.
11. Mendoza-Dominguez, A.; Russell, A.G. *Atmos. Environ.* **2001**, *35*, 2879-2894.
12. Harley, R.A.; Russell, A.G.; McRae, G.J.; Cass, G.R.; Seinfeld, J.H. *Environ. Sci. Technol.* **1993**, *27*, 378-388.
13. Frank, I.E.; Friedman, J.H. *Technometrics* **1993**, *35*, 109-148.
14. Yang, Y.-J.; Wilkinson, J.G.; Russell, A.G. *Environ. Sci. Technol.* **1997**, *31*, 2859-2868.
15. Pielke, R.A.; Cotton, W.R.; Walko, R.L.; Tremback, C.J.; Lyons, W.A.; Grasso, L.D.; Nicholls, M.E.; Moran, M.D.; Wesley, D.A.; Lee, T.J.; Copeland, J.H. *Meteor. Atmos. Phys.* **1992**, *49*, 69-91.
16. Wilkinson, J.G.; Loomis, C.F.; McNally, D.E.; Emigh, R.A.; Tesche, T.W. *Technical Formulation Document: SARMAP/LMOS Emissions Modeling System (EMS-95)*; AG-90/TS26 & AG-90/TS27; Alpine Geophysics: Pittsburgh, PA, 1994.
17. Odman, M.T.; Russell, A.G. *J. Geophys. Res.* **1991**, *96*, 7363-7370.
18. Kumar, N.; Odman, M.T.; Russell, A.G. *J. Geophys. Res.* **1994**, *99*, 5385-5397.
19. Odman, M.T.; Russell, A.G. *Atmos. Environ.* **1991**, *25A*, 2385-2394.
20. Odman, M.T.; Russell, A.G. *Atmos. Environ.* **1993**, *27A*, 793-799.
21. Odman, M.T.; Russell, A.G. In *Air Pollution Modelling and Its Applications XII*; Gryning, S.-E., Batchvarova, E., Eds.; Plenum: New York, 2000; pp 651-660.
22. Carter, W.P.L. *Atmos. Environ.* **1990**, *24*, 481-518.

23. Carter, W.P.L. *Atmos. Environ.* **1996**, *30*, 4275-4290.
24. Berkowitz, C.M.; Easter, R.C.; Scott, B.C. *Atmos. Environ.* **1989**, *23*, 1555-1571.
25. Boylan, J.; Wilkinson, J.; Yang, Y.-J.; Odman, T.; Russell, A. Particulate Matter and Acid Deposition Modeling for the Southern Appalachian Mountains Initiative. In *Proceedings of the 93rd Annual Meeting & Exhibition of A&WMA*, Salt Lake City, UT, June 2000; Air & Waste Management Association: Pittsburgh, PA, 2000; Paper No. 707.
26. Nenes, A.; Pandis, S.N.; Pilinis, C. *Aquat. Geochem.* **1998**, *4*, 123-152.
27. Pandis, S.N.; Harley, R.A.; Cass, G.R.; Seinfeld, J.H. *Atmos. Environ.* **1992**, *26A*, 2269-2282.
28. Wesely, M.L. *Atmos. Environ.* **1989**, *23*, 1293-1304.
29. Odman, T.; Boylan, J.; Wilkinson, J.; Yang, Y.-J.; Russell, A.; Doty, K.; McNider, R. Ozone Modeling for the Southern Appalachians Mountains Initiative. In *Proceedings of the 93rd Annual Meeting & Exhibition of A&WMA*, Salt Lake City, UT, June 2000; Air & Waste Management Association: Pittsburgh, PA, 2000; Paper No. 698.
30. Kalnay, E.; Kanamitsu, M.; Kistler, R.; Collins, W. *Bull. Am. Meteor. Soc.* **1996**, *77*, 437-471.
31. Geron, C.D.; Pierce, T.E.; Guenther, A.B. *Atmos. Environ.* **1995**, *29*, 1569-1578.
32. McNair, L.A.; Harley, R.A.; Russell, A.G. *Atmos. Environ.* **1996**, *30*, 4291-4301.
33. Myers, R.H. *Classical and Modern Regression with Applications*, 2nd ed.; Duxbury: Belmont, CA, 1990.
34. Chang, M.E.; Hartley, D.E.; Cardelino, C.; Chang, W.-L. *Geophys. Res. Lett.* **1996**, *23*, 3007-3010.
35. Harley, R.A.; Sawyer, R.F.; Milford, J.B. *Environ. Sci. Technol.* **1997**, *31*, 2829-2839.
36. National Research Council. *Modeling Mobile-Source Emissions*; National Academy Press: Washington, DC, 2000.
37. Seigneur, C.; Pun, B.; Pai, P.; Louis, J.-F.; Solomon, P.; Emery, C.; Morris, R.; Zahniser, M.; Worsnop, D.; Koutrakis, P.; White, W.; Tombach, I. *J. Air & Waste Manage. Assoc.* **2000**, *50*, 588-599.
38. Gruber, M.H.J. *Improving Efficiency by Shrinkage: The James-Stein and Ridge Regression Estimators*; Statistics: Textbooks and Monographs, Vol. 156; Marcel Dekker: New York, 1998.

About the Authors

Alberto Mendoza-Dominguez (corresponding author) is an assistant professor in the Chemical Engineering Department, Instituto Tecnológico y de Estudios Superiores de Monterrey (ITESM), Monterrey Campus, Ave. Eugenio Garza Sada 2501 Sur, Monterrey, N.L., Mexico, 64849; e-mail: almendoz@campus.mty.itesm.mx. Armistead G. Russell is the Georgia Power Professor of Environmental Engineering, School of Civil and Environmental Engineering, Georgia Institute of Technology, 200 Bobby Dodd Way, Atlanta, GA 30332-0512; e-mail: trussell@themis.ce.gatech.edu.